



Label-free electrochemical lead (II) aptasensor using thionine as the signaling molecule and graphene as signal-enhancing platform



Feng Gao, Cai Gao, Suyu He, Qingxiang Wang*, Aiqun Wu

College of Chemistry and Environment, Fujian Province Key Laboratory of Modern Analytical Science and Separation Technology, Minnan Normal University, Zhangzhou 363000, PR China

ARTICLE INFO

Article history:

Received 22 November 2015

Received in revised form

29 January 2016

Accepted 30 January 2016

Available online 17 February 2016

Keywords:

Lead ion

Aptasensor

Graphene

Thionine

ABSTRACT

A label-free and highly sensitive electrochemical aptasensor for Pb^{2+} was constructed using thionine (TH) as the signaling molecule and graphene (GR) as the signal-enhancing platform. The electrochemical sensing interface was fabricated by stepwise assembly of GR and TH on the lead (II) specific aptamer (LSA) modified electrode. Upon interaction with Pb^{2+} , the aptamer probe on the sensor underwent conformational switch from a single-stranded DNA form to the G-quadruplex structure, causing the GR with assembled TH released from the electrode surface into solution. As a result, the electrochemical signal of TH on the aptasensor was substantially reduced. Under the optimal experimental conditions, the attenuation of peak currents presented a good linear relationship with the logarithm of Pb^{2+} concentrations over the range from 1.6×10^{-13} to 1.6×10^{-10} M. The detection limit was estimated to be 3.2×10^{-14} M. The aptasensor also exhibited good regenerability, excellent selectivity, and acceptable reproducibility, indicating promising application in environment monitoring of lead.

© 2016 Elsevier B.V. All rights reserved.

1. Introduction

Lead ion (Pb^{2+}) is one of the most well-known highly toxic metallic pollutants that possess serious threat to the environment and human health even at a low concentration level (Lee et al., 2009; Nigg et al., 2008). For example, it is a demonstrated fact that Pb^{2+} can cause long-term damage to various systems of the body, including the nervous system, reproductive system, brain, kidney, liver and many other organs (Li et al., 2009). Therefore, the development of simple and robust approach for the routine detection of Pb^{2+} in drinking water, food, air, and soil is of considerable significance for environment and food safety monitoring.

Up to date, diverse methods had been exploited for the analysis of Pb^{2+} , which included atomic absorption/emission spectrometry (Deo and Godwin, 2000), surface plasmon resonance (Pelossof et al., 2012), inductively coupled plasma mass spectrometry (ICP-MS) (Aydin and Soyak, 2010), chemical/optical sensor (Shenashen et al., 2013; Khairy et al., 2013), etc. Although these methods are reliable and accurate, many of them suffered from the limitations of expensive instruments, sophisticated sample preparation processes, low sensitivity and serious matrix interference, which greatly limit their practical applications, especially on-line and fast analysis. Alternatively, electrochemical methods possessed the

advantages of low-cost, high selectivity and simple instrument, providing a promising protocol for the high-powered determination of Pb^{2+} . Anodic stripping voltammetry (ASV) is a convenient electrochemical method for Pb^{2+} detection (Sopha et al., 2014; Wang et al., 2013). However, the strict requirements for test conditions, complicated absorption process and the intermetallic disturbing for the stripping peak limit the practical application of this electrochemical method.

Aptamers are a type of functional artificial oligonucleotides with high affinity with various target molecules including small molecules, metal ions, proteins and even the entire cells (Ellington and Szostak, 1990). In the past few years, they attracted great attention in sensor construction due to their excellent properties such as good stability, ease of synthesis and modification, high binding specificity (Gao et al., 2014; Pang et al., 2015). The guanine-rich oligonucleotide has been developed as a lead (II) specific aptamer (LSA) (Li et al., 2010; Zang et al., 2014). After binding with Pb^{2+} , the free coil-like LSA will transform to stable G-quadruplex (G4) structure. Based on this fact, the LSA has been frequently exploited as a specific identification element to build the elegant and robust sensors for selective detection of Pb^{2+} . Among them, the electrochemical G4-based aptasensors received more and more attention for Pb^{2+} detection because it integrates the advantages of both electrochemical technology and aptamer (Lin et al., 2011; Li et al., 2011; Jarczewska et al., 2015). However, these sensors commonly suffered from the following drawbacks: (1) High background response caused by the non-selective

* Corresponding author.

E-mail address: axiang236@126.com (Q. Wang).

interaction of electroactive probe (like $\text{Fe}(\text{CN})_6^{3-/4-}$ or MB) with the LSA produced a low signal-to-noise ratio; (2) Low binding amount of redox probe to G4-Pb^{2+} complex resulted in inferior signal production; (3) Similar binding of K^+ and Pb^{2+} with LSA give rise to the poor selectivity of the sensors. Therefore, it is still a challenge to develop novel sensing strategy for high-performance determination of Pb^{2+} .

Graphene (GR), a single layer of carbon atoms bonded together in a hexagonal lattice, has been widely used in the preparation of electrochemical biosensor in recent years due to its remarkable properties such as a high surface area, excellent electron transport capability, low cost, and good biocompatibility (Wang et al., 2014a; Zhang et al., 2015a; Liu et al., 2014). It has been reported that various biological probes such as single-stranded DNA (ssDNA), antibodies and aromatic compounds can adsorb on the surface of GR by means of π - π interactions and/or Vander Waals' force (Zhang et al., 2011; Min et al., 2011; Ni et al., 2012). The unique GR/ssDNA interaction has shown fascinating applications including gene diagnosis, protein analysis, and intracellular tracking (Lu et al., 2009; Huang et al., 2013). Thionine (TH), an aromatic redox dye has been widely used as an electroactive probe in the field of electroanalytical chemistry, because of its unique advantages such as high water solubility, reversible electrochemical response and modest redox potential (Ma et al., 2015; Yang et al., 2014). Owing to its planar aromatic structure, thionine molecules have also been demonstrated to be capable of adsorbing onto the surface of GR via strong π - π stacking and synergistically noncovalent charge transfer (Chen et al., 2011).

Herein we constructed a novel label-free electrochemical aptasensor for Pb^{2+} by using GR as the signal molecule carrier, and TH as the signaling probe. The GR was first adsorbed onto the surface of LSA modified electrode through hydrophobic and π - π stacking interactions. Then the electroactive TH molecules were assembled at the electrode surface through π - π interaction with GR layer. When the LSA was interacted with Pb^{2+} , the LSA was transformed from the free coil state to the stable G4 structure, from which the GR with the adsorbed TH was released from the electrode surface, resulting in the reduction of electrochemical response. Such a process is label-free, which greatly improved the convenience for the fabrication of the aptasensor. In addition, the GR on the electrode surface not only acted as a bridge to link the LSA probe and the TH signal molecules, but also greatly enhanced electrochemical signal of the sensor due to its large surface area effect and high electronic conductivity. The anti-interference ability of the sensor, especially for K^+ was also improved by the presence of the GR in the sensing layer. Under the optimal experimental conditions, there is a linear relationship between the attenuation of peak currents of TH and the logarithm of Pb^{2+} concentrations over the range from 1.6×10^{-13} to 1.6×10^{-10} M. The detection limit was estimated to be as low as 3.2×10^{-14} M. This method could be potentially used for lead ion detection with high sensitivity and reliability.

2. Experimental

2.1. Materials and reagents

The thiol-modified LSA was purchased from Sangon Biotechnology Co., Ltd. (Shanghai, China) and its sequence was as follows: 5'-GGG TGG GTG GGT GGG T-C₆-SH-3'. Thionin, 6-mercapto-1-hexanol (MCH) and tris(2-carboxyethyl) phosphine hydrochloride (TCEP) were bought from Sigma-Aldrich (Shanghai, China). Graphite powder and all the metal salts including NaCl, CaCl_2 , $\text{MgCl}_2 \cdot 6\text{H}_2\text{O}$, ZnCl_2 , $\text{NiCl}_2 \cdot 6\text{H}_2\text{O}$, HgCl_2 , AgNO_3 , $\text{CuSO}_4 \cdot 5\text{H}_2\text{O}$, $\text{CdCl}_2 \cdot 2.5\text{H}_2\text{O}$, $\text{MnSO}_4 \cdot \text{H}_2\text{O}$, $\text{Co}(\text{CH}_3\text{COO})_2 \cdot 4\text{H}_2\text{O}$,

KNO_3 , $\text{Pb}(\text{NO}_3)_2$ were provided by Xilong Chemical Plant Co., Ltd. (Guangdong, China) and used directly without further purification. The other reagents, such as ethylenediaminetetraacetic acid disodium (EDTA), and tris(hydroxymethyl) aminomethane (Tris) were of analytical reagent grade and purchased commercially. Doubly distilled water (DDW) was used throughout the experiments. GR used in this experiment was prepared by chemical reduction of graphene oxide with hydrazine as described in literature (Hummer and Offeman, 1958). The dispersion of GR was prepared by adding 3 mg GR into 10 mL DMF, followed by ultrasonication for 3 h to obtain the uniform blank suspension. Before use, the solution was ultrasonicated for 30 min again.

The stock solutions of LSA (0.1 μM) was prepared with IB buffer solution (25 mM Tris-HCl, 100 mM NaCl, 100 mM MgCl_2 and 10 mM TCEP, pH 8.2) and kept frozen. Phosphate saline (PBS) was prepared by mixing 20 mM NaCl and 50 mM NaH_2PO_4 - Na_2HPO_4 . The supporting electrolyte used for electrochemical measurements was 20 mM Tris-HCl buffer (pH 7.0). Before measurements, all the electrolytes were purged with high-purity nitrogen for 30 min.

2.2. Instruments

Electrochemical measurements were carried out with CHI 650 C electrochemical workstation (Shanghai, China) at room temperature. A three-electrode system consisted of a bare or modified gold electrode (AuE, $\Phi=2.0$ mm in diameter) as the working electrode, a platinum wire as the counter electrode, and an Ag/AgCl (3 M KCl) as the reference electrode. Atomic Force Microscopy (AFM) for the sensor fabrication and Pb^{2+} binding process was carried out on a CSPM-5500 scanning probe microscope (China). The pH of all the solutions was measured on a Leici Model pHs25 digital acidometer (Shanghai, China). The ICP-MS detection of Pb^{2+} was performed on an Agilent model 7500cx analyzer (Tokyo, Japan). UV-vis spectra was carried out on Mapada Instruments Co., Ltd (Shanghai, China).

2.3. Fabrication of the aptasensor

The immobilization of LSA on AuE was achieved through a classical Au-S assembly chemistry. In brief, the AuE was first mechanically polished on 1.0 μm , 0.3 μm , and 0.05 μm alumina slurry, followed by ultrasonic clean in DDW, ethanol and DDW, in turn. Then the freshly polished electrode was dipped in piranha solution (98% H_2SO_4 /30% H_2O_2 , 7:3, V/V) for 30 min, and subsequently electrochemically scanned between -0.2 and $+1.5$ V in 0.5 M H_2SO_4 until stable CV curves were obtained. After being rinsed with DDW and dried with nitrogen, the cleaned electrode was immediately immersed into IB containing 0.1 μM LSA solution for 24 h at 4 °C. After that, the electrode was rinsed with PBS to remove the non-specifically adsorbed DNA, and the obtained electrode was denoted as LSA/AuE. Then, the resulted electrode was immersed into 1 mM MCH for 2 h to passivate the free interspaces between the LSA probes. The obtained electrode was denoted as MCH-LSA/AuE.

2.4. Step-by-step assembly of GR and TH

For assembly of GR, the prepared MCH-LSA/AuE was first immersed in 0.3 g L^{-1} GR for 125 min. Afterwards, the electrode was gently rinsed with DDW to remove the loosely attached GR, thus the GR assembled electrode (GR/MCH-LSA/AuE) was prepared. Then the electroactive molecules of TH were further attached onto sensing interface through incubating GR/MCH-LSA/AuE in 1.0 mM TH for 100 min. After careful washing with DDW, the TH adsorbed electrode (TH/GR/MCH-LSA/AuE) was achieved.

2.5. Pb^{2+} determination by the aptasensor

To detect Pb^{2+} ions, the TH adsorbed electrode (TH/GR/MCH-LSA/AuE) was initially incubated in 200 μ L solution containing desired concentration of Pb^{2+} for 60 min under room temperature. Then the electrode was immersed into 25 mM PBS solution for 10 min with gentle shaking to remove the nonspecifically adsorbed Pb^{2+} ions. Cyclic voltammetry (CV) was recorded in 20 mM pH 7.0 Tris–HCl at a scan rate of 0.1 $V s^{-1}$ between $-0.7 V$ and $+0.4 V$. Differential pulse voltammetry (DPV) was recorded in 20 mM pH 7.0 Tris–HCl within the potential range from $-0.4 V$ to 0 V with a pulse width of 0.05 s and a step potential of 4 mV.

2.6. Safety considerations

As the piranha solution and most of the tested metal ions are highly toxic and have adverse effects on human health, all the experiments involving these materials should be performed with protective gloves. The waste solutions containing heavy metal ions should be collectively reclaimed to avoid their pollution to the environment.

3. Results and discussion

3.1. Working principle of the proposed sensor

Fig. 1 depicts the working principle of the aptasensor on the basis of using TH as the signal molecule and GR as the signal amplification platform. First, the thiol modified LSA was self-assembled on the AuE surface via the classical Au–S bond to construct the Pb^{2+} recognition layer. Then, the electrode surface was blocked with MCH to form a mixing monolayer, through which the anchored LSA strands could be erected up to achieve the higher capture ability to Pb^{2+} and meanwhile the residue sites on the electrode surface could be occupied to avoid the non-specific adsorption of other substances. Followed by, the GR was assembled onto the MCH-LSA modified electrode based on the π -stacking interaction between the hexagonal cells of GR and the planar

structure of nucleobases (Pang et al., 2015). Then the aromatic electroactive molecules of TH were further adsorbed on the surface of GR also by the strong π - π interaction, resulting in a measurable electrochemical signal. When the analyte of Pb^{2+} was present in the test solution, the free LSA with the single-stranded coil structure on the electrode surface would be changed to the folded G4 structure through its specific interaction with Pb^{2+} . Thus, the affinity of GR with LSA would be significantly reduced, and as a result, the complex of GR with the electroactive TH would be liberated from the sensing interface, leading to the reduction of the redox signal of the sensor. Since the formation of G4 was specifically dependent on the presence of Pb^{2+} , the proposed sensor should respond to Pb^{2+} with high selectivity. On the other hand, the rational application of GR on the sensor construction not only enhances the attaching amount of TH by its outstanding surface effect, but also improves the electron transfer kinetic of TH on the electrode surface owing to its excellent conductivity, which made the signal intensity as well as sensitivity of the sensor being greatly improved.

3.2. Feasibility characterization and feasibility investigation of the Pb^{2+} aptasensor

Based on the successful fabrication of the sensing layer on AuE, the stepwise fabrication process of the Pb^{2+} aptasensor was first electrochemically characterized by CV and EIS using $Fe(CN)_6^{3-/4-}$ as the redox probe. The result and detailed discussion were presented in Supporting information (Fig. S-1). The electrochemical behaviors of the constructed sensor, and its response to the Pb^{2+} were investigated through CV studies. Fig. 2A shows the CVs of different electrodes in 20 mM Tris–HCl buffer (pH 7.0). As seen, not any redox peak was observed at MCH-LSA/Au (curve a) and GR/MCH-LSA/AuE (curve b), suggesting that the mixed modification layers of MCH-LSA and GR/MCH-LSA were electro-inactive under the measured conditions. However at the TH accumulated electrode (TH/GR/MCH-LSA/Au), two pairs of well-defined redox peaks were observed at $-0.102 V$ and $-0.213 V$, $0.162 V$ and $0.075 V$ (curve d), respectively, which was in accordance with the two-step single electron transfer process of TH in literatures (Lo et al., 2008).

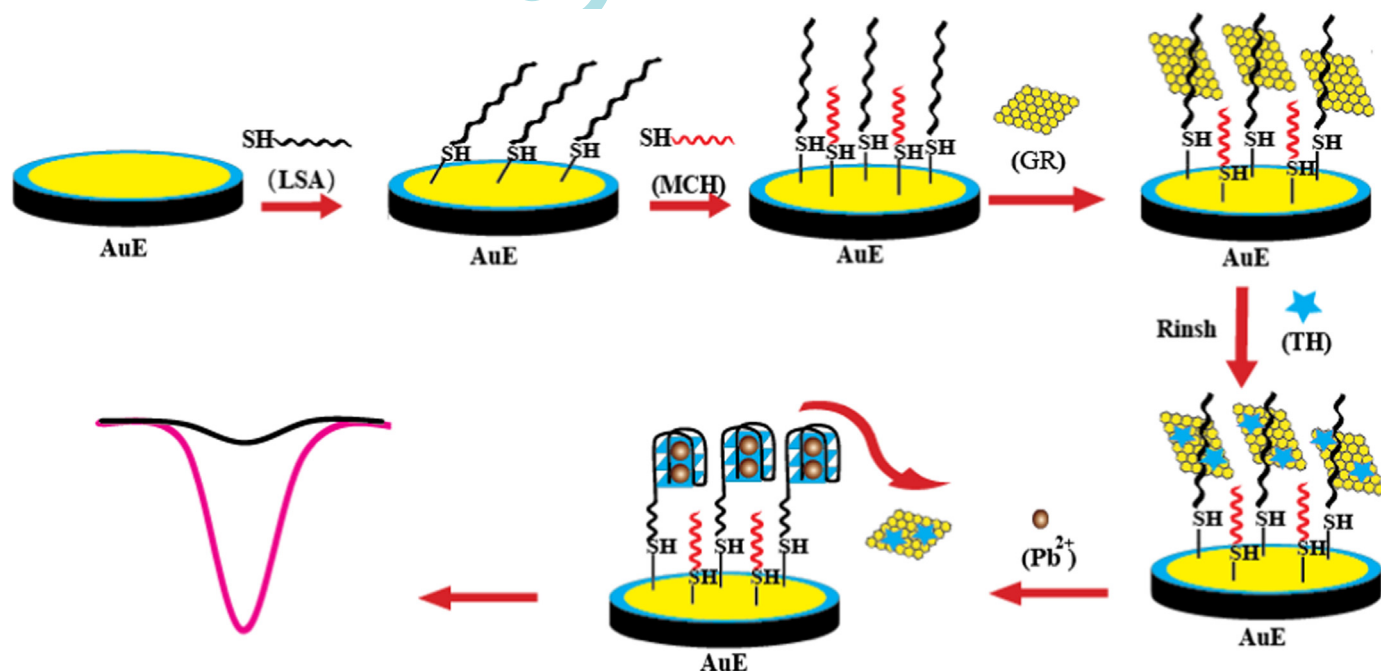


Fig. 1. Schematic representation of electrochemical Pb^{2+} aptasensor based on stepwise assembly of GR and TH on aptamer modified electrode surface.

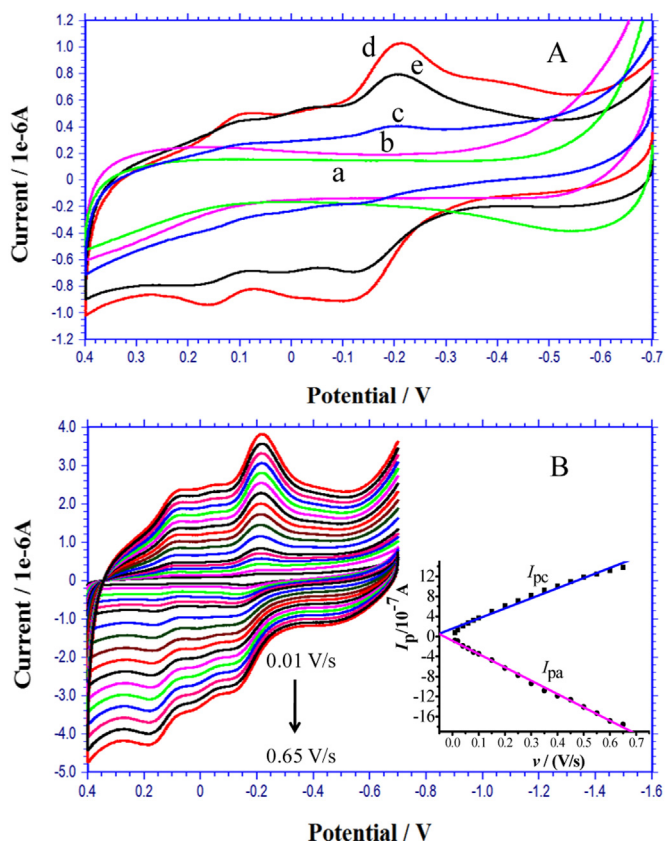


Fig. 2. (A) CVs of (a) LSA-MCH/AuE, (b) GR/LSA-MCH/AuE, (c) TH/LSA-MCH/AuE, (d) TH/GR/LSA-MCH/AuE before and (e) after incubation in 1.0×10^{-8} M Pb^{2+} solution in 20 mM Tris-HCl (pH 7.0) at a scan rate of 0.1 V/s. (B) CVs of 1.0 mM TH/GR/LSA-MCH/AuE in 20 mM Tris-HCl at different scan rates. Inset: plot of peak current (I_p) versus scan rate (ν).

This result demonstrated that the electroactive molecule of TH had been attached to the surface of GR/MCH-LSA/AuE, and displayed good electrochemical response. The scan rate (ν) experiments further revealed that the redox peaks of TH enhanced regularly with the increase of the scan rate (Fig. 2B), and both the oxidation peak currents (I_{pc}) and reduction peak currents (I_{pc}) presented good linear relationships with the scan rate in the range from 0.01 V/s to 0.65 V/s (inset in Fig. 2B): I_{pc} (10^{-7} A) = $1.5653 + 20.2236 \nu$ (V/s) and I_{pa} (10^{-7} A) = $-0.8378 - 26.5998 \nu$ (V/s) with the correlation coefficients (r) of -0.9931 and 0.9984 , respectively, which is a typical adsorption-controlled process (Heli et al., 2004). This further suggested that TH had been adsorbed onto the surface of GR/LSA-MCH/AuE.

As a control, the electrochemical response of TH on the electrode without pre-assembly of GR (LSA-MCH/AuE) was also investigated (curve c). The result showed that the redox signal of TH at this electrode was obviously smaller than that on GR/MCH-LSA/AuE (curve d). This indicated that the adsorbed GR played an important role to enhance the electrochemical response of the sensor likely due to its surface area effect and high electronic conductivity. In addition, after the sensor (TH/GR/MCH-LSA/AuE) was incubated in 1.0×10^{-8} M Pb^{2+} solution for 60 min, and then measured under the same conditions, it was found that the electrochemical signal of the aptasensor decreased significantly (curve e), demonstrating that large amount of the surface-bound TH had been liberated from the electrode surface. This confirmed that after interaction with Pb^{2+} , the free coil strands of LSA were transformed to the rigid G4 structure, leading to the dissociation of TH-GR complex from the sensor surface. These changes also experimentally indicated that the concept relying on the different

affinity of TH-GR with Pb^{2+} -free and Pb^{2+} -bound forms of LSA is feasible for monitoring Pb^{2+} .

In order to further probe the fabrication process and detection feasibility of the biosensor, the atomic force microscopy (AFM) was applied to characterize the different electrode. The results were displayed in Fig. S-2 in Supporting information. As seen, a relative smooth surface with the height difference of 6.26 nm was observed for MCH-LSA/AuE (A). When the electrode was assembled with GR, it was found that the electrode become coarse, and the height difference was increased to 68.36 nm (B), confirming the successful adsorption of GR. After TH molecules were further adsorbed on the electrode surface, the surface morphology of the electrode become much coarser with a height difference of 137.98 nm (C). Meanwhile some white dots were appeared, which could be ascribed to the aggregation of the adsorbed TH molecules on the GR surface. However, after the sensing interface was interacted with Pb^{2+} , the surface roughness of the electrode significantly decreased with the height difference of 55.82 nm and the white dots disappeared (D), suggesting that the complex of GR and TH had been stripped from the electrode. It was noticeable that the height difference (nm) of Pb^{2+} -bound electrode was still larger than that of MCH-LSA/AuE. This might be attributed to the fact that when LSA was interacted with Pb^{2+} , the rigid G4 structure was formed on the electrode surface, resulting in higher height difference than that on coil-like LSA modified electrode.

3.3. Surface density of adsorbed TH and the average binding ratio of TH to LSA

In the conventional electrochemical aptasensors, one aptamer probe strand was only tagged with one signal molecule, which resulted in small electrochemical signal as well as low sensitivity of the sensors (Baker et al., 2006; Jiang et al., 2015). In this work, the GR was used as a loading platform for the electroactive TH molecules, thus it could be imaged that the adsorption amount of the signal molecules could be greatly increased by the surface area effect of the nano-sized GR. In order to testify this result, the adsorbing amount of TH and the average binding of TH to LSA were calculated. From the CV diagram of TH/GR/LSA-MCH/AuE in Tris-HCl buffer as showed in curve d of Fig. 2A, the total reduction charge amount (Q) of TH at the electrode surface was estimated to be $13.6 \mu\text{C}$ according to the following formula: (Laviron, 1979) $I_p = nFQ\nu/4RT$, where n is the electron-transfer number of TH, F Faraday's constant, R universal gas constant, T Kelvin temperature. Then based on the formula of $\Gamma = NQ/nFA$ (where N is the Avogadro's constant, A the geometric area of AuE), the surface density (Γ_{TH}) of adsorbed TH at the electrode surface was yielded to be 4.9×10^{-10} mol cm^{-2} . Fig. S-2 shows the typical CC curves of MCH/MSA/Au in Tris-HCl buffer solution without (curve a) and with $50 \mu\text{M}$ $[\text{Ru}(\text{NH}_3)_6]^{3+}$ (curve b). The surface density of the LSA (Γ_{LSA}) was then calculated to be 6.1×10^{-11} mol cm^{-2} according to the literature (Steel et al., 1998). Thus, the average binding ratio of TH to LSA ($\Gamma_{\text{TH}}/\Gamma_{\text{LSA}}$) was determined to be 8.1, namely each aptamer afford eight electroactive signal molecules in average, which is significantly larger than the traditional electroactive aptamer with single electroactive tag (Baker et al., 2006; Jiang et al., 2015; Zhang et al., 2015b). This increased absorption amount of the signal molecule is helpful to improve the sensitivity of the developed sensor.

3.4. Optimization of the experimental conditions

In order to achieve the superior sensitivity of the Pb^{2+} aptasensor, some experimental conditions such as incubation time (t_{GR}) of LSA-MCH/AuE in GR dispersion, accumulation time (t_{TH}) of TH at the electrode surface, accumulation concentration (C_{TH}) of

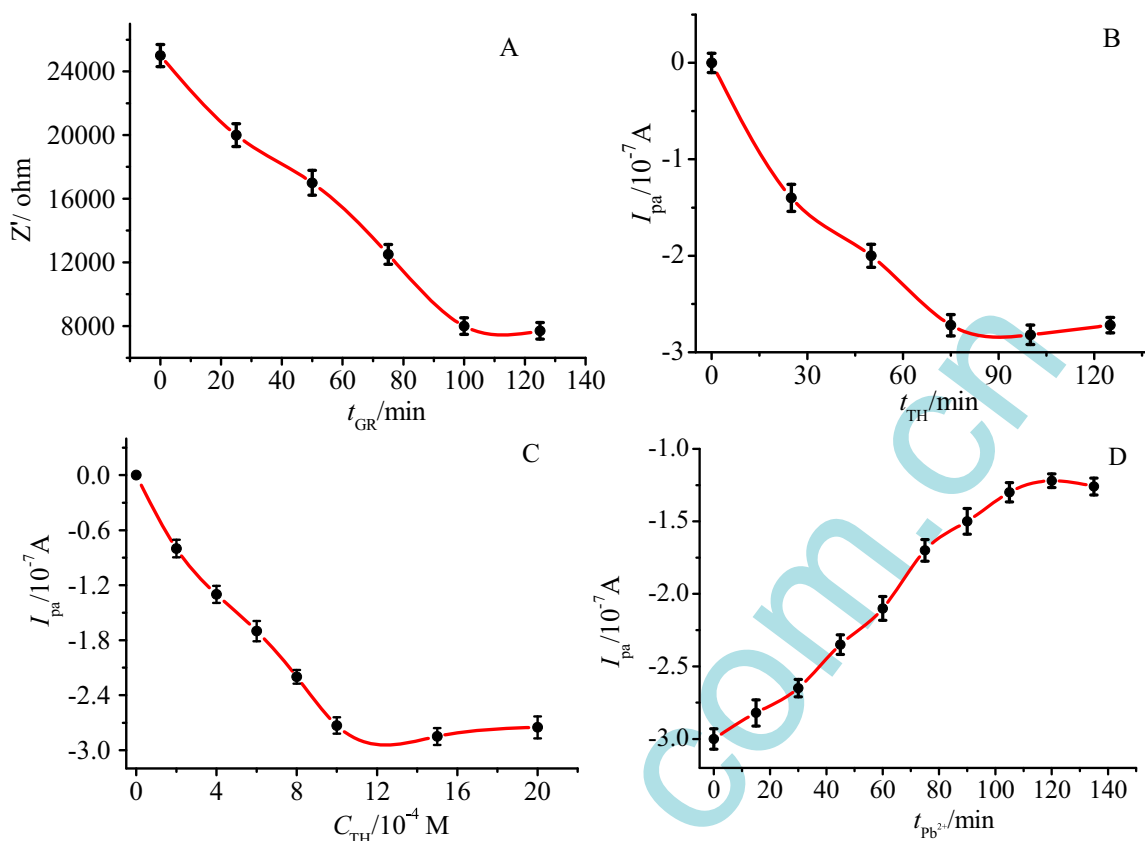


Fig. 3. (A) Relationship of electron transfer resistance (R_{et}) versus incubation time of LSA-MCH/AuE in GR dispersion. (B) and (C) showed the relationship of oxidation peak currents (I_{pa}) versus accumulation time (t_{TH}) accumulation concentrations (C_{TH}) of TH on GR/LSA-MCH/AuE. (D) Relationship of I_{pa} versus accumulation time ($t_{Pb^{2+}}$) of Pb^{2+} on TH/GR/LSA-MCH/AuE. The concentration of Pb^{2+} is 1.0×10^{-8} M.

TH, and the reaction time of Pb^{2+} (t_{Pb}) were optimized. The adsorption of GR on LSA-MCH/AuE was investigated by EIS using $Fe(CN)_6^{3-/4-}$ couple as the electroactive probe. Fig. 3A showed the relationship of electron transfer resistance (R_{et}) versus the t_{GR} . It was found that with the increase of t_{GR} , the R_{et} values decreased gradually, showing that more and more GR was adsorbed on LSA-MCH/AuE and accelerated the electron transfer kinetic of $Fe(CN)_6^{3-/4-}$ redox couple on the electrode surface. When the time reached to 100 min, the R_{et} values were hardly changed, suggesting that GR had been adsorbed on the electrode surface at a saturation level. Fig. 3B shows the plot of the oxidation peak (I_{pa}) of TH on the GR/LSA-MCH/AuE versus t_{TH} . As seen, the I_{pa} values of TH increased with the values of t_{TH} up to 100 min, and then to be constant, suggesting the adsorption saturation of TH at GR/LSA-MCH/AuE. Therefore, 100 min was chosen as the optimal incubation time for TH. The effect of the accumulation concentration (C_{TH}) of TH on the response signal of the sensor showed that the I_{pa} values of TH increased with the increase of C_{TH} in the range from 0.2 mM to 1.0 mM, and then leveled off when the concentration was upon 1.0 mM (Fig. 3C). So, 1.0 mM was selected as the optimal accumulation concentration of TH in the following studies. Fig. 3D shows the relationship of I_{pa} values versus the reaction time of the sensor with Pb^{2+} ($t_{Pb^{2+}}$). It was observed that with the increase of reaction time, the I_{pa} value decreased gradually, indicating that more and more Pb^{2+} -induced G4 structure had been formed on the electrode surface. When the time was upon 100 min, the I_{pa} became a constant, which was an indication of the binding equilibrium between LSA and Pb^{2+} . Therefore, 100 min was selected as the optimal time for Pb^{2+} binding in this work.

3.5. Analytical performance of the aptasensor

Under the optimized conditions, the analytical performance of the developed sensor to Pb^{2+} was assessed by DPV. Fig. 4A shows the DPVs of TH/GR/MCH-LSA/AuE upon interaction with different concentrations of Pb^{2+} ($C_{Pb^{2+}}$). As seen, the oxidation peaks of TH decreased gradually with the increased of Pb^{2+} concentration, testifying that the electrochemical response of the sensor is dependent on the concentration of Pb^{2+} . The inset in Fig. 4B reveals a linear correlation between the oxidation peak currents (I_{pa}) of TH and the logarithm value of $C_{Pb^{2+}}$ ($\log C_{Pb^{2+}}$) over the range from 1.6×10^{-13} to 1.6×10^{-10} M. The linear regression equation was I_{pa} (10^{-7} A) = $2.69 \log(C_{Pb^{2+}}/M) + 0.434$, with a correlation coefficient (R) of -0.9909 . The detection limit was estimated to be 3.2×10^{-14} M based on the signal to noise ratio ($S/N=3$), which was significantly lower than that of other LSA-based electrochemical approaches (Table S-1 in Supporting information). Such a low detection limit could be attributed to use of GR with large surface area for loading large amount of electroactive TH and ultrahigh electron transfer ability for enhancing the electrochemical signal intensity of TH.

The selectivity of the electrochemical sensor was investigated by examining the response of the developed sensor to the other ions including Co^{2+} , Zn^{2+} , Mg^{2+} , K^+ , Ag^+ , Cu^{2+} , Ni^{2+} , Ca^{2+} , Hg^{2+} , Cd^{2+} and Mn^{2+} that possibly coexisting with Pb^{2+} . The results were summarized in Fig. 5A. As displayed, the sensor has a large DPV peak current difference (ΔI_{pa}) in the response to Pb^{2+} , but hardly exhibited substantial signal variation to the other metal ions, suggesting that the protocol developed in this work possessed excellent selectivity. It was noticeable that many previous literatures have reported that the G-rich oligonucleotide could also

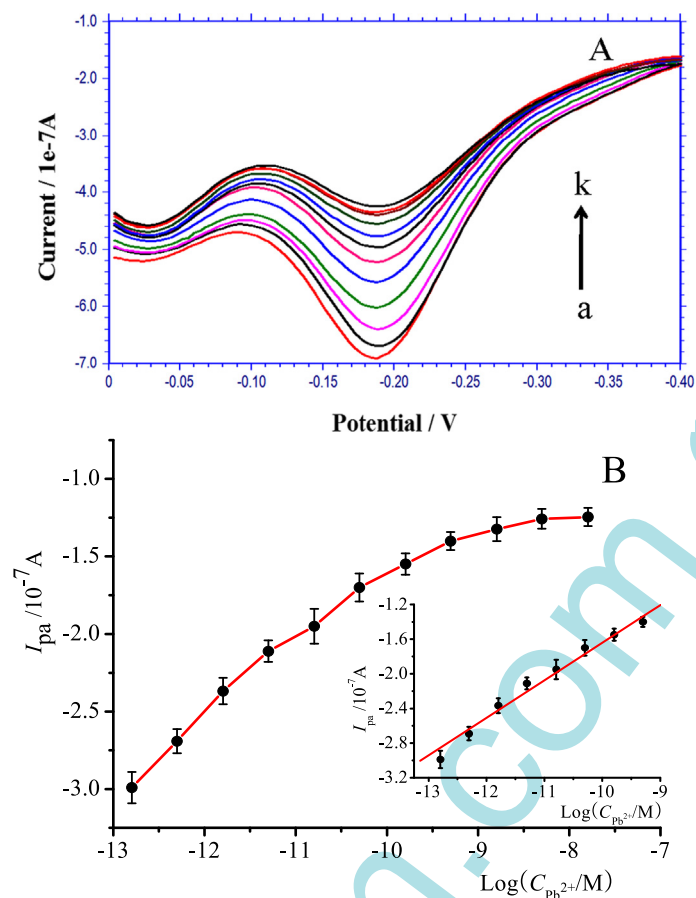


Fig. 4. (A) Dependence of DPVs of the aptasensor on Pb^{2+} concentrations: (a) 0, (b) 1.6×10^{-13} , (c) 5.0×10^{-13} , (d) 1.6×10^{-12} , (e) 5.0×10^{-12} , (f) 1.6×10^{-11} , (g) 5.0×10^{-11} , (h) 1.6×10^{-10} , (i) 5.0×10^{-10} , (j) 1.6×10^{-9} , (k) 5.0×10^{-9} , (l) 1.6×10^{-8} M in 20 mM Tris-HCl (pH 7.0) buffer. (B) The calibration curve of DPV peak current as a function of Pb^{2+} concentration. The inset shows the linear relationship part between the I_{pa} versus $\text{Log } C_{\text{Pb}^{2+}}$.

be induced to form quadruplex structure by the K^+ (Wang et al., 2014b; Aleman-Garcia et al., 2014). However in this work the sensor did not show obvious DPV change in the presence of K^+ . This might be related to the fact that Pb^{2+} had the higher association

force with LSA than the K^+ , and the ingenious use of GR in this protocol: After GR was adsorbed on electrode surface through π -stacking with LSA, the K^+ is hard to induce the conformation switch of LSA from free coil state to G4 structure, therefore the

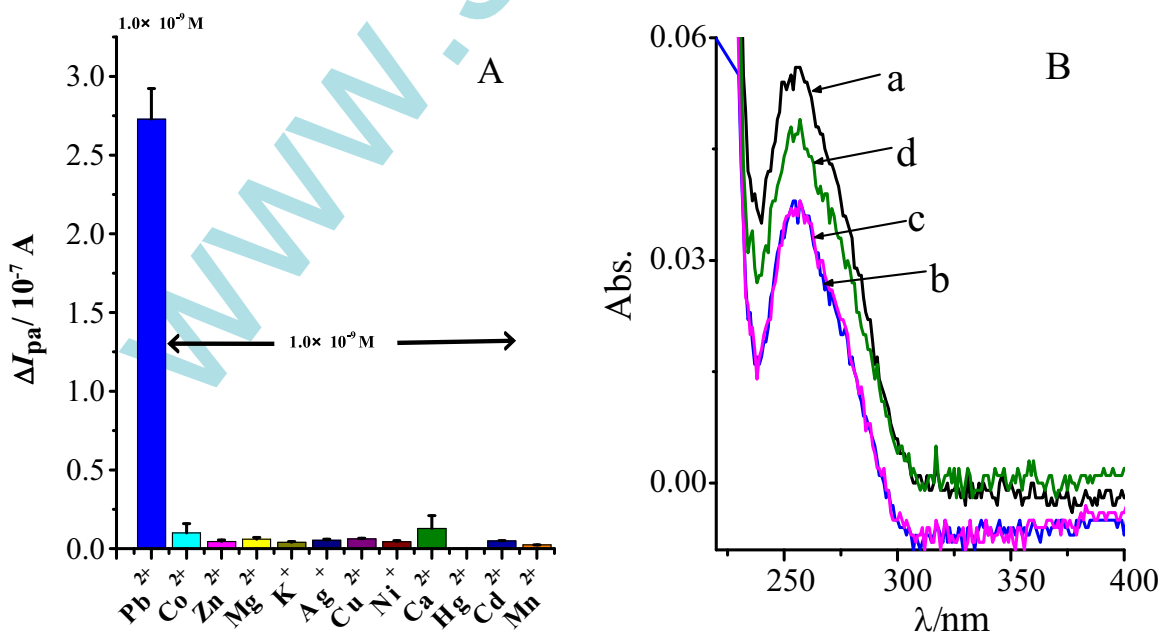


Fig. 5. (A) Electrochemical response value (ΔI_{pa}) of the sensor to different ions. All concentrations of metal ions are 1.0×10^{-9} M. (B) the UV spectra of LSA (a), LSA-GR mixture before (b) and after adding K^+ (c) and Pb^{2+} (d).

Table 1
Determination of Pb^{2+} in water samples using the developed aptasensor and ICP-MS^a.

Samples	Developed aptasensor (nM)	ICP-MS method (nM)	Relative deviation (%)
River water 1	24.36 ± 4.67	26.09 ± 5.45	−6.63
River water 2	29.39 ± 5.12	27.25 ± 3.76	7.85
Tap water 1	11.51 ± 3.62	12.29 ± 4.57	6.34
Tap water 2	13.45 ± 3.49	14.19 ± 5.13	−5.21

^a All values were obtained as average of three repetitive determinations plus standard deviation

sensor remained the original electrochemical signal. However, the Pb^{2+} had the higher efficiency for stabilizing G4 structure of LSA, therefore when the sensor was interacted with Pb^{2+} , the GR with TH could be effectively removed from the electrode surface, resulting in the decrease of electrochemical signal.

In order to testify this speculation, the effect of K^+ and Pb^{2+} on the structure change of GR bound LSA was investigated by UV spectra. Fig. 5B shows the UV spectra of LSA–GR mixture before and after adding K^+ or Pb^{2+} . As seen, LSA showed an obvious peak at 260 nm due to the characteristic absorption of the bases (curve a). When GR was added to the LSA solution to form LSA–GR complex, it was founded that the adsorption peak decreased significantly, which could be explained by the π – π coupling between LSA and GR (curve b). In the presence of K^+ , the intensity of the absorption peak was hardly changed, indicating that the K^+ could not change the situation of the LSA–GR (curve c). However, when the complex was added with Pb^{2+} , an obvious increase of the adsorption peak was observed, suggesting that some LSA strands had been dissociated from the LSA–GR complex. This result confirmed that Pb^{2+} had a higher affinity than K^+ with LSA to form G4.

3.6. Regenerability, reproducibility and stability of the aptasensor

Regenerability, reproducibility and stability are important indexes to evaluate the performance of a sensor (Du et al., 2014; Wang et al., 2015). The regenerability of the sensor was investigated by immersing the Pb^{2+} -bound electrode into 1.0 mM EDTA at room temperature for 80 min, washing with DDW, and then re-assembly with GR and TH. Figure S-3 in Supporting Information shows the peak currents of the aptasensor during the first five regeneration runs, from which it could be observed that only slight decrease of the oxidation peak current (I_p) in DPV after five runs of regeneration, showing that the sensor could be facily regenerated. In addition, five independent sensors were prepared and examined. The relative standard deviation (RSD) of 7.9% was obtained for the oxidation peak currents of the five sensors, indicating that the developed sensor had good reproducibility. The stability of the developed sensor also investigated by keeping the electrode in the fridge at 4 °C and recording its current response each day. In the first week, only 9.1% loss in the current signal was observed, showing excellent stability of the sensor.

3.7. Analysis of Pb^{2+} in real water samples

The practical use of the developed electrochemical aptasensor for Pb^{2+} determination in real samples were evaluated by determination of Pb^{2+} in tap water of our campus and Jiu Longjiang river of our city. The samples were first filtered through a 0.22 μm membrane to remove the suspended solids. Then, they were analyzed with the proposed method and ICP-MS. The results were summarized in Table 1. It was found that the results from the two approaches are consistent as judged from the relative deviation

< 7.85%. This also indicated that the developed method had outstanding accuracy for Pb^{2+} in real sample detection.

4. Conclusions

In this paper, we report a new electrochemical aptasensor for Pb^{2+} based on the specific binding of the LSA towards the Pb^{2+} and the unique π -stacking of LSA/GR and GR/TH. The constructed aptasensor is lable-free, and take advantage of the unique properties of GR, such as high surface area, strong adsorption to electroactive TH, and outstanding electrocatalysis, which is helpful to enhance the electrochemical response intensity and the sensitivity of the sensor. The detection limit was estimated to be as low as 3.2×10^{-14} M. The aptasensor also exhibited good regenerability, excellent selectivity, and acceptable reproducibility. When the sensor was applied for the detection of Pb^{2+} in the real water samples, the results were comparable with the ICP-MS method, indicating promising application in environment monitoring of lead. Such a strategy could also be extended to the other sensors such as immunosensors and aptasensors

Acknowledgments

The work is supported by the National Natural Science Foundation of China (No. 21275127), and Program for New Century Excellent Talents in Fujian Province University (No. JA12204)

Appendix A. Supplementary material

Supplementary data associated with this article can be found in the online version at <http://dx.doi.org/10.1016/j.bios.2016.01.096>.

References

- Aleman-Garcia, M.A., Orbach, R., Willner, I., 2014. Chem. -Eur. J. 20, 5619–5624.
- Aydin, F.A., Soylak, M., 2010. J. Hazard. Mater. 173, 669–674.
- Baker, B.R., Lai, R.Y., Wood, M.S., Doctor, E.H., Heeger, A.J., Plaxco, K.W., 2006. J. Am. Chem. Soc. 128, 3138–3139.
- Chen, C., Zhai, W.T., Lu, D.D., Zhang, H.B., Zheng, W.G., 2011. Mater. Res. Bull. 46, 583–587.
- Deo, S., Godwin, H.A., 2000. J. Am. Chem. Soc. 122, 174–175.
- Du, J., Yue, R., Ren, F., Yao, Z., Jiang, F., Yang, P., Du, Y., 2014. Biosens. Bioelectron. 53, 220–224.
- Ellington, A.D., Szostak, J.W., 1990. Nature 346, 818–822.
- Gao, C., Wang, Q.X., Gao, F., Gao, F., 2014. Chem. Commun. 50, 9397–9400.
- Heli, H., Bathaie, S.Z., Mousavi, M.F., 2004. Electrochem. Commun. 6, 1114–1118.
- Huang, J., Zong, C., Shen, H., Cao, Y., Ren, B., Zhang, Z., 2013. Nanoscale 5, 10591.
- Hummer, W.S., Offeman, R.E., 1958. J. Am. Chem. Soc. 80, 1339.
- Jarczewska, M., Kierzkowska, E., Ziolkowski, R., Górski, L., Malinowska, E., 2015. Bioelectrochemistry 101, 35–41.
- Jiang, B., Li, F., Yang, C., Xie, J., Xiang, Y., Yuan, R., 2015. Anal. Chem. 87 (5), 3094–3098.
- Khairy, M., El-Safty, S.A., Shenashen, M.A., Elshehy, E.A., 2013. Nanoscale 5, 7920–7927.
- Laviron, E., 1979. J. Electroanal. Chem. Interfacial Electrochem. 100, 263–270.
- Lee, H.Y., Bae, D.R., Park, J.C., Song, H., Han, W.S., Jung, J.H., 2009. Angew. Chem. Int. Ed. Engl. 48, 1239–1243.
- Li, F., Feng, Y., Zhao, C., Tang, B., 2011. Chem. Commun. 47, 11909–11911.
- Li, T., Dong, S., Wang, E., 2010. J. Am. Chem. Soc. 132, 13156–13157.
- Li, X., Zhang, Y., Tan, M., Liu, J., Bao, L., Zhang, G., Li, Y., Iida, A., 2009. J. Environ. Sci. 21, 1118–1124.
- Lin, Z., Chen, Y., Li, X., Fang, W., 2011. Analyst 136, 2367–2372.
- Liu, J., Wang, X., Wang, T., Li, D., Xi, F., Wang, J., Wang, E., 2014. ACS Appl. Mater. Interfaces 6, 19997–20002.
- Lo, P.H., Kumar, S.A., Chen, S.M., 2008. Colloid Surf. B66, 266–273 (2008).
- Lu, C.H., Yang, H.H., Zhu, C.L., Chen, X., Chen, G.N., 2009. Angew. Chem. 121, 4879–4881.
- Ma, M., Miao, Z., Zhang, D., Du, X., Zhang, Y., Zhang, C., Lin, J., Chen, Q., 2015. Biosens. Bioelectron. 64, 477–484.
- Min, S.K., Kim, W.Y., Cho, Y., Kim, K.S., 2011. Nat. Nanotechnol. 6, 162–165.

- Ni, G., Wang, Y., Wu, X., Wang, X., Chen, S., Liu, X., 2012. *Immunol. Lett.* 2, 126–132.
- Nigg, J.T., Knottnerus, G.M., Martel, M.M., Nikolas, M., Cavanagh, K., Karmaus, W., Rappley, M.D., 2008. *Biol. Psychiatry* 63, 325–331.
- Pang, Y., Rong, Z., Xiao, R., Wang, S., 2015. *Sci. Rep.* 5, 9451.
- Pelossof, G., Tel-Vered, R., Willner, I., 2012. *Anal. Chem.* 84, 3703–3709.
- Shenashen, M.A., El-Safty, S.A., Elshehy, E.A., 2013. *J. Hazard. Mater.* 260, 833–843.
- Sopha, H., Roche, J., Švancara, I., Kuhn, A., 2014. *Anal. Chem.* 86, 10515–10519.
- Steel, A.B., Herne, T.M., Tarlov, M., 1998. *J. Anal. Chem.* 70, 4670–4677.
- Wang, G.F., Chen, L., Zhu, Y.H., He, X.P., Xua, G., Zhang, X.J., 2014a. *Biosens. Bioelectron.* 61, 410–416.
- Wang, J., Yang, B., Wang, H., Yang, P., Du, Y., 2015. *Anal. Chim. Acta* 893, 41–48.
- Wang, L., Xu, W.H., Yang, R., Zhou, T., Hou, D., Zheng, X., Liu, J.H., Huang, X.J., 2013. *Anal. Chem.* 85, 3984–3990.
- Wang, X., Wang, Q., Wang, Q., Gao, F., Yang, Y., Guo, H., 2014b. *ACS Appl. Mater. Interfaces* 6, 11573–11580.
- Yang, C., Dou, B., Shi, K., Chai, Y., Xiang, Y., Yuan, R., 2014. *Anal. Chem.* 86 (23), 11913–11918.
- Zang, Y., Lei, J., Hao, Q., Ju, H., 2014. *ACS Appl. Mater. Interfaces.* 6, 15991–15997.
- Zhang, M., Liao, C., Mak, C.H., You, P., Mak, C.L., Yan, F., 2015a. *Sci. Rep.* 5, 8311.
- Zhang, P., Wu, X., Yuan, R., Chai, Y., 2015b. *Anal. Chem.* 87 (6), 3202–3207.
- Zhang, Z., Huang, H., Yang, X., Zang, L., 2011. *J. Phys. Chem. Lett.* 2, 2897–2905.

www.spm.com.cn